

Physicochemical Characterization of Two Polysulfon-Amides in Dilute Solution

Ye Chen,¹ Di Wu,¹ Jun Li,² Shenghui Chen,² Xiaofeng Wang,² Yumei Zhang,^{*1} Huaping Wang¹

Summary: As one class of high temperature resistant aromatic polymers, polysulfonamides (PSA) are widely used in industry, physicochemical properties and conformation in solution have not been disclosed yet. In this work, the dilute solution behaviour of poly(*m*-diphenylsulphone terephthal amide) (*m*-PSA) was investigated by laser light scattering (LLS) and viscometry. The results showed that the *m*-PSA exists as single chains both in dimethylsulfoxide (DMSO) and dimethylformamide (DMF). The value of radius of gyration to hydrodynamic radius (s/R_h) indicates that the *m*-PSA has a random coil conformation in solution. Both the persistence length a and the characteristic ratio C_∞ indicate that the *m*-PSA chain is flexible in solution. The Mark-Houwink equation of *m*-PSA in DMSO was determined as $[\eta] = 1.62 \times 10^{-5} M_w^{0.87}$, and the exponent of 0.87 supports the assumption that *m*-PSA forms random coils in DMSO-solution at 25 °C. It was found that the flexibility of the PSA was affected when 4,4'-diphenylsulphone terephthalamide monomer was incorporated in backbone. The PSA random copolymer (*r*-PSA) with a comonomer ratio of 3:1 (4,4'-diaminodiphenylsulfone to 3,3'-diaminodiphenylsulfone) also had a random coil conformation in DMF; the rigidity increased, while the mobility of the chain was maintained.

Keywords: conformation; flexibility; intrinsic viscosity; laser light scattering; polysulfonamide

Introduction

Since the commercialization of poly(*m*-phenyleneisophthalamide) (PMIA) which has a trade name NOMEX (Dupont USA), high temperature resistant aromatic fibers have developed rapidly. A series of heat-resistant fibers, such as poly(*p*-phenylene terephthalamide) (PPTA), polybenzimidazole (PBI), poly(*p*-phenylenebenzobisoxazole) (PBO), polyphenylene sulfide (PPS), and polyetheretherketone (PEEK), have been synthesized and applied in aerospace, civil engineering, construction,

protective apparel, geotextiles and electronic areas. [1,2]

As one type of such polymers, polysulfonamides (PSA) have been synthesized by polycondensation of diaminodiphenylsulfone with terephthaloyl chloride or isophthaloyl chloride at low temperature. [3,4] Because of its good solubility and spinnability [5] from some polar organic solvents such as *N,N*-dimethylacetamide (DMAc), dimethylformamide (DMF) and dimethylsulfoxide (DMSO), PSA fibers have been commercialized under the trade name TANLON (Shanghai Tanlon Fiber Co., Ltd) and been used to for protective textiles, filters, and insulation materials. Due to the existence of the additional sulfonyl ($-\text{SO}_2-$) in its backbone, PSA fibers exhibit excellent flame retardancy and thermal stability in the decomposition temperature higher than 420 °C. [6]

¹ State Key Laboratory for Modification of Fiber Materials, College of Material Science and Engineering, Donghua University, Shanghai, 201620, China
Fax: +86-21-67792957;
E-mail: zhangym@dhu.edu.cn

² Shanghai Tanlon Fiber Co., Ltd, Shanghai, 201419, China

However, the knowledge of the basic physicochemical properties of PSA is still limited. Previously the physicochemical characterization of some aromatic polyamides has been reported and material properties of different backbone structures have been reported.^[7] It is known that flexibility is usually poor if an aromatic ring is incorporated in the backbone, for instance poly(*p*-phenylene terephthalamide), poly(*p*-phenylenebenzo bisoxazole), and polybenzimidazole are all rigid polymers.^[8] However, the flexibility of aromatic polymers can be changed by varying the chemical structure or the configuration. For example, the polymer chain of poly(*p*-phenylene terephthalamide) is highly rigid, while the poly(*m*-phenyleneisophthalamide) chain is highly flexible in DMAc/LiCl solution.^[9] The difference is caused by the different chain structure. In the poly(*m*-phenyleneisophthalamide) backbone whose covalent bonds were not conjugated, the amide groups are linked with *m*-phenylene, and the potential energy of internal rotation is low. Thus the chain is more flexible. On the contrary, amide groups in poly(*p*-phenylene terephthalamide) backbone are linked to *p*-phenylene and π - π conjugate structures are formed. Thus the chain is more rigid. In addition, flexibility and solubility of aromatic polymers are enhanced if flexible groups such as oxy (–O–), sulfonyl (–SO₂–) or sulfanediyl (–S–) are incorporated in the backbone.^[10–12]

The solution behaviour of *m*-PSA in DMF and DMSO has been studied by means of viscometry and laser light scattering (LLS) including both static light scattering (SLS) and dynamic light scattering (DLS) to characterize the conformation

and flexibility of *m*-PSA. The relation between $[\eta]$ and M_w of *m*-PSA in DMSO has been established by the Mark-Houwink equation. Conformation and flexibility of a PSA copolymer (*r*-PSA) with comonomer ratio 3:1 has also been investigated.

Experimental Part

Materials

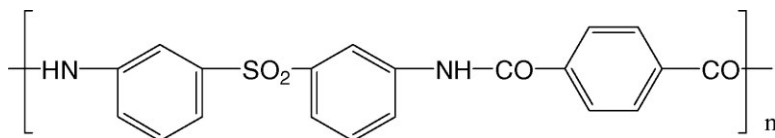
m-PSA, provided by Shanghai Tanlon Fiber Co., Ltd, was synthesized by polycondensation with 3,3'-diaminodiphenylsulfone (3,3'-DDS) and Terephthaloyl chloride (TPC) in DMAc at low temperature (generally at 0 °C). NMR results proved the structure of the polysulfoneamide samples (*m*-PSA). The structure is shown in Scheme 1, and the *m*-PSA samples used in this paper are summarized in Table 1.

r-PSA, also provided by Shanghai Tanlon Fiber Co., Ltd, was synthesized by polycondensation of 4,4'-diaminodiphenylsulfone (4,4'-DDS), 3,3'-DDS and TPC, with a monomer ratio 3:1:4 in DMAc at low temperature. The NMR results showed that all products had the expected structure, which is shown in Scheme 2.

DMF was purchased from Tianjin Shield Company. DMSO was purchased from Beijing Yilireagent Company. The solvents were redistilled before used. Both *m*-PSA and *r*-PSA dissolved easily in these solvents at room temperature.

LLS

A commercial spectrometer from Brookhaven Instruments Corporation (BI-200SM Goniometer, Holtsville, NY) was used for SLS and DLS over a scattering angular range of 20–120°. A solid-state laser



Scheme 1.
structure of *m*-PSA.

Table 1.

Intrinsic viscosity $[\eta]$ and molecular weight of different *m*-PSA samples in DMSO detected from LLS measurement.

Sample	$[\eta](\text{dL/g})$	k'	k''	$M_w \times 10^{-5}$ (LLS)
<i>m</i> -PSA-1	1.52	0.54	0.11	5.1
<i>m</i> -PSA-2	1.23	0.29	0.19	4.1
<i>m</i> -PSA-3	1.31	0.58	0.06	4.6
<i>m</i> -PSA-4	0.88	0.32	0.17	2.8

k' -Huggins constant

k'' -Kramer constant

emitting vertically polarized light (CNI Changchun GXC-III, 532nm, 100Mw) operating at 532nm was used as the light source, and a BI-Turb^oCorr Digital Correlator was used to collect and process data. In SLS measurements, the time-averaged excess scattered intensity at angle θ , also known as the Rayleigh ratio $R_{vv}(q)$, was related to the weight-averaged molar mass M_w , the Z-averaged root mean square radius s , the second virial coefficient A_2 , and the scattering vector q as,

$$\frac{Hc}{R_{vv}(q)} \approx \frac{1}{M_w} \left(1 + \frac{1}{3} s^2 |q|^2 \right) + 2A_2c \quad (1)$$

where $H = 4\pi^2 n^2 (dn/dc)^2 / (N_A \lambda_0^4)$ and $q = (4\pi n / \lambda) \sin(\theta/2)$, with N_A , n , (dn/dc) and λ_0 being the Avagadro constant, the refractive index of the solvent, the specific refractive index increment of the solution, and the wavelength of light in vacuum, respectively. The dn/dc values of PSA in DMF and DMSO were determined using a BI-DNDC differential refractometer (Brookhaven, NY) equipped with a laser at 535nm. For *m*-PSA in DMF, dn/dc was found to be $0.195 \pm 0.004 \text{ cm}^3/\text{g}$ at room temperature; in DMSO it was $0.167 \pm 0.007 \text{ cm}^3/\text{g}$. For *r*-PSA in DMF, it was $0.211 \pm 0.008 \text{ cm}^3/\text{g}$.

In DLS the intensity-intensity time autocorrelation function $G^{(2)}(t, \theta)$ was measured in the self-beating mode. It is related to the normalized first order electric field time correlation function $g^{(1)}(t, \theta)$ as $G^{(2)}(t, \theta) = A [1 + \beta |g^{(1)}(t, \theta)|^2]$, where A is the measured base line, β is a spatial coherence factor, t is the delay time, and θ is the scattering angle. $G^{(1)}(t, \theta)$ is further related to the line width distribution $G(\Gamma)$. The normalized distribution function $G(\Gamma)$ of the characteristic line width was obtained using a Laplace inversion program, CONTIN^[13]. The line width Γ is a function of both concentration and scattering vector q , which can be expressed as

$$\Gamma/q^2 = D_0(1 + k_d C) [1 + f(sq)^2] \quad (2)$$

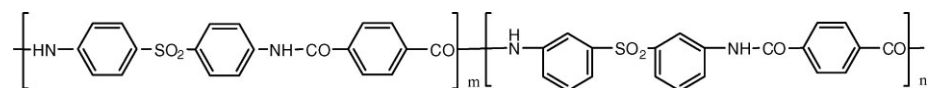
With D_0 , k_d , f being the translational diffusive coefficient, the diffusion second virial coefficient, and a dimensionless constant, respectively. D_0 can be further converted into the hydrodynamic radius R_h by using the Stokes-Einstein equation:

$$D_0 = \frac{k_B T}{6\pi\eta R_h} \quad (3)$$

where k_B , T , and η are the Boltzmann constant, the absolute temperature, and the viscosity of the solvent respectively. All LLS measurements were conducted at $T = 25 \pm 0.1^\circ\text{C}$.

Viscosity Measurement

The viscosity of the PSA solution was measured at $T = 25 \pm 0.1^\circ\text{C}$ with an Ubbelohde viscometer using the dilution method. PSA was dissolved in DMSO at 25°C and diluted to four concentrations from 5.0 mg/ml to 2.5 mg/ml. Huggins and Kraemer plots were used to obtain the

**Scheme 2.**

structure of *r*-PSA ($m:n = 3:1$).

intrinsic viscosity $[\eta]$, according to:

Huggins equation:

$$\frac{\eta_{sp}}{c} = [\eta] + k' [\eta]^2 c \quad (4)$$

Kramer equation:

$$\frac{\ln \eta_r}{c} = [\eta] - k'' [\eta]^2 c \quad (5)$$

Where η_{sp} , η_r , k' , k'' are the specific viscosity, the relative viscosity, Huggins constant and Kramer constant respectively, and c is the polymer concentration. The kinetic energy correction was always negligible.

Results and Discussion

LLS studies of *m*-PSA Dilute Solution

Figure 1 shows the Zimm plot of *m*-PSA-4 in DMSO at 25 °C. The radius of gyration s obtained was 27.8 nm. With the measured value of dn/dc , a molecular weight $M_w = 2.8 \times 10^5$ g/mol and the second virial coefficient $A_2 = 4.8 \times 10^{-4}$ mol · mL/g² were obtained for *m*-PSA-4 in DMSO. Similar results were obtained with the other samples of *m*-PSA; they are summarized in Table 1. In DMF solutions, the results are slightly different, for example, $s = 28.6$ nm, $M_w = 2.3 \times 10^5$ g/mol and $A_2 = 5.3 \times 10^{-4}$ mol · mL/g² for *m*-PSA-4. The results indicate that DMF and DMSO should have a similar solvation state with PSA due to the similar polarity. The positive values of A_2 indicate that DMSO and DMF are both good solvents for *m*-PSA, and provide direct evidence that *m*-PSA is molecularly dispersed in DMSO and DMF.

The persistence length a and the characteristic ratio C_∞ , which are generally used to represent the chain flexibility, could be calculated based on the results from SLS. The persistence lengths a of *m*-PSA in DMSO and DMF were calculated by the Benoit-Doty equation:^[14]

$$s^2 = a^2 \left[\frac{L}{3a} - 1 + \frac{2a}{L} - \frac{2a^2}{L^2} \left(1 - e^{-\frac{L}{a}} \right) \right] \quad (6)$$

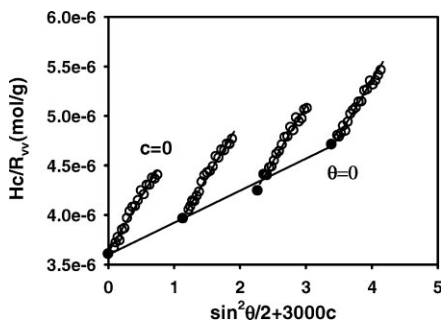


Figure 1.

Zimm plot of *m*-PSA-4 in DMSO at 25 °C.

where L is the contour length, displaying the length of fully stretched chain in all-trans conformation. The length of repeating unit in *m*-PSA was obtained from computer simulation (ChemSketch). As shown in Figure 2, the length of the *m*-PSA unit is about 1.628 nm. The side width and the verticality of *m*-PSA obtained were 0.551 nm and 0.235 nm, respectively. The simulation showed that the three benzene rings of the repeating unit are not in-line and twisted in an angle, due to the free rotation of the C–N, C–C, C–S single bond. Using the unit length of 1.628 nm, we calculated the contour length of *m*-PSA-4 with $M_w = 2.8 \times 10^5$ g/mol to about 1.2 μm. The persistence length was calculated to be 2.1 nm for *m*-PSA-4 in DMSO, and to 2.7 nm in DMF. The small value of persistence length indicates that *m*-PSA has flexible chains in these solvents, the same as the result of poly(*m*-phenyleneisophthalamide) in DMAc/LiCl solvent.^[9]

In order to further show the flexibility of PSA in solvent, the characteristic ratio C_∞ was determined according to:

$$C_\infty = \frac{\langle r^2 \rangle_0}{nl^2} \quad (7)$$

with $\langle r^2 \rangle_0$, n and l being the unperturbed end-bend distance, the number of main-chain bonds and the bond length, respectively. As we known $\langle r^2 \rangle_0 = 6 \langle s^2 \rangle_0$, and the radius of gyration in the unperturbed state $\langle s^2 \rangle_0^{1/2}$ could be obtained by $\langle s^2 \rangle_0^{1/2} = \langle s^2 \rangle^{1/2} / \alpha_s$. The linear expansion factor α_s can be

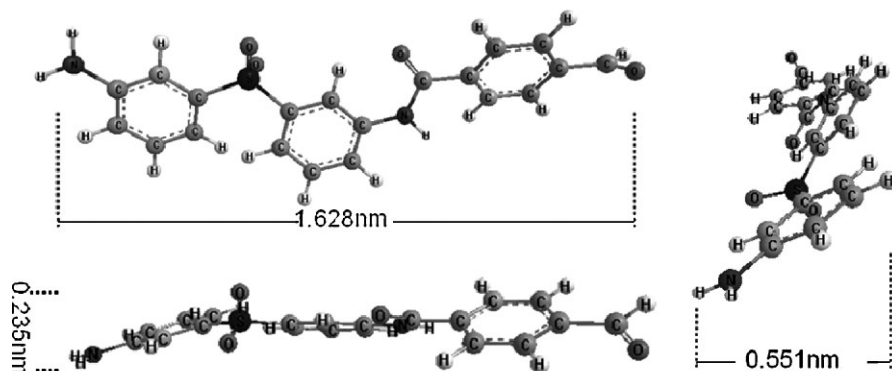


Figure 2.
simulation of *m*-PSA unit.

obtained from M_w , A_2 , and $\langle s^2 \rangle^{1/2}$ using a penetration function ψ derived by the Kurata-Fukatsu-Sotobayashi-Yamakawa theory (KFSY).^[15]

$$\psi = zh_0(z) \\ = (0.746 \times 10^{-25}) A_2 M^2 / \langle s^2 \rangle^{3/2} \quad (8)$$

Where $h_0(z) = 1 - (1 + 3.903z)^{-0.468} / 1.828$, and $\alpha_s = 1 + 1.78z$. The expansion factor α_s of *m*-PSA-4 in DMSO and DMF was 1.11 and 1.09 respectively. And the value of C_∞ for *m*-PSA-4 in DMSO was about 2.0 while 2.6 in DMF which again indicates that *m*-PSA has flexible chains. With the assumption of a freely rotating chain of *m*-PSA in these solvents, the rotation angle could be obtained according to:

$$C_\infty = \frac{1 + \cos\theta}{1 - \cos\theta} \quad (9)$$

Using the calculated value of C_∞ , the rotation angle was about 70° in DMSO and 64° in DMF. We propose that though benzene rings are the main structural element in *m*-PSA, the existence of C–N, C–C, C–S single bond and the asymmetry of *m*-phenyle in backbone facilitated internal rotation in the molecules. The chemical defects or twists as well as an inherent torsional flexibility reduce the chain stiffness,^[16] so *m*-PSA exists as flexible chains and with defined rotation angle in dilute solution.

Figure 3 shows the DLS results of *m*-PSA-4 in DMSO at a concentration of 0.6 mg/mL. Similar results were observed in DMF/PSA solutions. As shown in Figure 3, a monomodal distribution was observed at scattering angles from 30° to 90° , which indicates that *m*-PSA exists as single chains in these solvents and no aggregation or association occurred. Figure 4(a) showed the power law scaling of Γ vs q^2 . The plot is linear and passes through the origin, which indicates that the relaxation mode of *m*-PSA in the solvent is diffusive. The plot in Figure 4(b) shows the translation diffusion coefficient D as a function of concentration yielding a limiting diffusion coefficient in infinite dilution, D_0 , of $1.8 \times 10^{-11} \text{ m}^2/\text{s}$. According to the Stokes-Einstein relation, eq. 3, the hydrodynamic radius R_h of *m*-

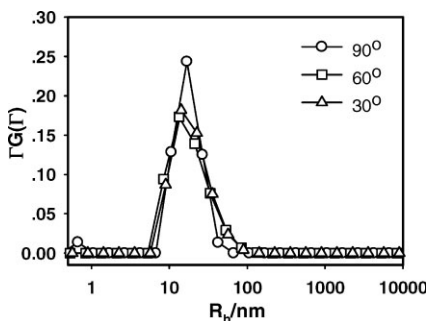


Figure 3.
Size distribution of *m*-PSA-4 in DMSO at 0.6 mg/mL at different scattering angles.

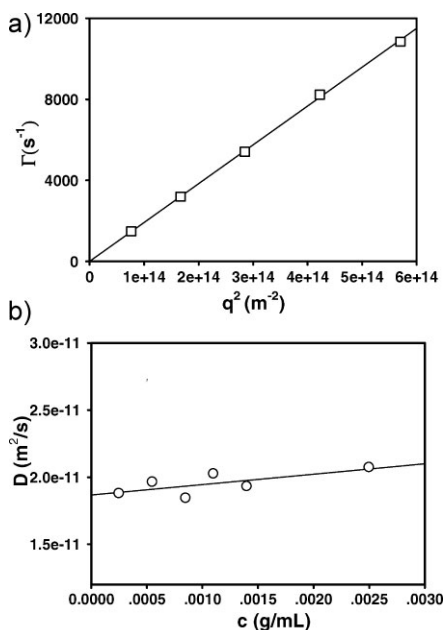


Figure 4.

Angular dependence of the average characteristic line-width of relaxation of *m*-PSA-4 in DMF at 1.4 mg/mL (a) and D as a function of concentration (b).

PSA-4 in DMF (15.6) and DMSO (15.8) was obtained. It has been established in the literature that the s/R_h ratio is closely related to the interaction between particle and solvent molecules, and can be used to estimate the conformation of polymers in solvents.^[17] The s/R_h value of *m*-PSA in DMF and DMSO were both about 1.8, which indicates that single *m*-PSA chain is in random coil conformation in these two solvents. In addition, the dispersity could be estimated from the size distribution to 1.67 for *m*-PSA-4.

Mark-Houwink Equation of *m*-PSA in DMSO

Figure 5 contains a Huggins plot and Kramer plot for *m*-PSA-2 in DMSO at 25 °C. The values of intrinsic viscosity $[\eta]$, Huggins constant k' and Kramer constant k'' were determined from the intercept and the slope of each plot; they are summarized in Table 1.

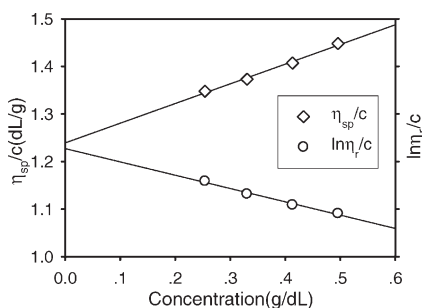


Figure 5.

Reduced viscosity (η_{sp}/c) and $\ln\eta_r/c$ dependences of concentrations (c) of *m*-PSA-2 in DMSO at 25 °C.

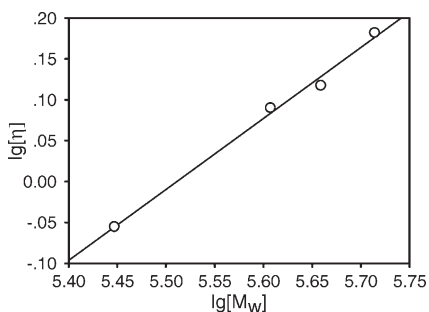


Figure 6.

M_w dependence of $[\eta]$ for *m*-PSA in DMSO at 25 °C.

The M_w dependence of $[\eta]$ for *m*-PSA in DMSO is plotted in Figure 6, and the Mark-Houwink equation:

$$[\eta] = KM_w^\alpha \quad (10)$$

may be well established in the M_w region from 2.8×10^5 to 5.1×10^5 , and the relationship was given:

$$[\eta] = 1.62 \times 10^{-5} M_w^{0.87} \quad (11)$$

The exponent value (α) is related to the shape of the macromolecules and the nature of the solvent. Usually, for a random polymer coil in a poor solvent the value of α is between 0.5 and 0.8. While in good solvent, the macromolecular chain becomes more expanded the value of α is between 0.8 and 1.0. The value α of *m*-PSA in DMSO is 0.87 is in agreement with the conformation of a random coil in a good solvent.

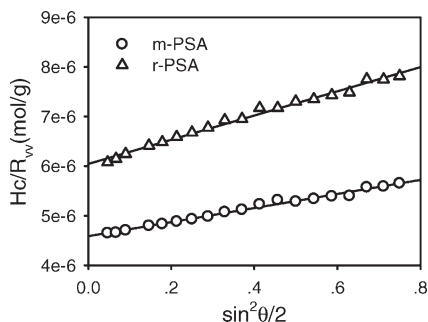


Figure 7.

Angular dependence of $(Hc/R_{vv})_{c=0}$ of *m*-PSA and *r*-PSA in DMF at 25 °C.

Conformation of *r*-PSA in Solvent

On the basis of the different structure between 3,3'-DDS and 4,4'-DDS monomer, the flexibility of *m*-PSA chain would be changed when 4,4'-DDS monomer was incorporated. Figure 7 shows the angular dependence of $(Hc/R_{vv})_{c=0}$ of *m*-PSA and *r*-PSA in DMF. The slope of the *r*-PSA plot is higher than for *m*-PSA, which means that the radius of gyration *r*-PSA chain is larger than for *m*-PSA. The LLS results of *r*-PSA are summarized in Table 2. For calculation of the persistence length we use the unit length 1.689 nm of *p*-phenylsulphone terephthalamide (calculated from simulation) and a contour length 0.8 μm for *r*-PSA. The DLS measurement showed that *r*-PSA is single chain in DMF, and the R_h of these two polymers were similar (data not shown). The *s* value of *r*-PSA is bigger than for *m*-PSA, while the molecular weight is smaller. The s/R_h ratio of *r*-PSA is 2.1, a little higher than that of *m*-PSA. This can be explained with two arguments. Incorporation of 4,4'-DDS increases the rigidity of the PSA chain as confirmed by the higher persistence length and characteristic ratio. On the other hand, the higher dispersity of

r-PSA increases the value of the s/R_h ratio.^[17] The dispersity of *r*-PSA is about 1.96, which was calculated from the R_h distribution. Though the rigidity increased, *r*-PSA was also flexible, as indicated by the small persistence length. This polymer is a random copolymer, and it is not possible to form a continuous para linked conjugated structure in whole chain.

Conclusion

Both homopolymer (*m*-PSA) and copolymer (*r*-PSA) exist as single chains in DMSO and DMF. The Mark-Houwink equation for *m*-PSA in DMSO at 25 °C was $[\eta] = 1.62 \times 10^{-3} M_w^{0.87}$ in the M_w region from 2.8×10^5 to 5.1×10^5 . In view of *a*, C_∞ , and s/R_h , both *m*-PSA and *r*-PSA have random coil conformation and are flexible. The flexibility of PSA was affected when 4,4'-DDS was part of the chain, and the *r*-PSA chain was more rigid than *m*-PSA although still a flexible chain. We propose that there are some *p*-phenylsulphone terephthalamide sequences formed in *r*-PSA chain, which increase rigidity. But *r*-PSA still has flexible chains in DMF and DMSO. Our future work is to investigate the flexibility and conformation of different PSA copolymers with various composition and to explore how the 4,4'-DDS structure influences the flexibility of PSA polymers.

Acknowledgements: This work was financially supported by Shanghai Science and Technology Commission (09JC1400800), National Natural Science Foundation of China (50873025), Shanghai Municipal Education Commission (10ZZ44), and the innovation funds for Ph.D students (Ye Chen) of Donghua University.

We would like to thank Prof. Liang of Peking University and Li Zhang of test center of Donghua University for providing the measurement of LLS.

Table 2.

LLS results of different PSA samples in DMF at 25 °C.

sample	$M_w \times 10^{-5}$	<i>s</i> (nm)	R_h (nm)	s/R_h	<i>a</i> (nm)	C_∞
<i>m</i> -PSA	2.3	28.6	15.8	1.8	2.7	2.6
<i>r</i> -PSA	1.8	32.3	15.4	2.1	4.3	4.1

[1] H. H. Yang, "Aromatic high-strength fibers", Wiley-Interscience, USA 1989, p. 33.

[2] B. Serge, F. Xavier, *Fire Mater.*, **2002**, 26, 155.

[3] S. A. Sundet, W. A. Murphey, S. B. Speck, *J. Polym. Sci.*, **1959**, 40, 389.

- [4] R. C. Evers, G. F. L. Ehlers, *J. Polym. Sci. Part A*, **1967**, 5, 1797.
- [5] R. Q. Ni, L. Chen, Z. F. Liu, H. F. Wang, X. F. Wang, *Synthetic Fiber in China*, **2005**, 6, 6.
- [6] X. F. Wang, Y. H. Zhang, *China Textile Leader*, **2005**, 1, 19.
- [7] L. H. Gan, P. Blais, D. J. Carlsson, T. Suprunchuk, D. M. Wiles, *J. Appl. Polym. Sci.*, **1975**, 19, 69.
- [8] J. J. Wang, H. Y. Wang, S. L. Zhang, H. H. Zhang, Y. Zhao, *J. Phys. Chem. B*, **2007**, 111, 6181.
- [9] D. Harwood, H. Aoki, Y. Lee, J. F. Fellers, J. L. White, *J. Appl. Polym. Sci.*, **1979**, 23, 2155.
- [10] X. F. Dai, X. L. You, X. W. Wang, Y. T. Cao, Z. F. Liu, *Materials Review*, **2004**, 18, 304.
- [11] Y. Oishi, S. Harada, M. Kamimoto, Y. Imai, *J. Polym. Sci. Pol. Chem.*, **1989**, 27, 3393.
- [12] Y. S. Negi, U. Razdan, V. Saran, *J. Macromol. Sci. R. M. C.*, , 39, 391.
- [13] S. W. Provencher, *Comput. Phys. Commun.*, **1982**, 27, 229.
- [14] H. Benoit, P. Doty, *J. Phys. Chem.*, **1954**, 57, 958.
- [15] M. Kurata, M. Fukatsu, H. Sotobayash, H. Yamakawa, *J. Chem. Phys.*, **1964**, 41, 139.
- [16] P. M. Cotts, T. M. Swager, Q. Zhou, *Macromolecules*, **1996**, 29, 7323.
- [17] W. Brown, “*Light Scattering: principles and development*”, Oxford University Press, New York 1996, p. 439.